Capture, encryption, compression, and display of digital holograms of three-dimensional objects

Unnikrishnan Gopinathan,[a] David S. Monaghan,[a] Alison E. Shortt,[b]
Thomas J. Naughton,[b] John T. Sheridan,[a] and Bahram Javidi[c]

[a]Department of Electronic and Electrical Engineering, University College Dublin,
Belfield, Dublin 4, Ireland
[b]Department of Computer Science, National University of Ireland, Maynooth,
County Kildare, Ireland
[c]Electrical and Computer Engineering, University of Connecticut,
371 Fairfield Road, Unit 1157, Storrs, CT 06269, USA

ABSTRACT

Digital holography can be used to capture the whole Fresnel field from a reflective or transmissive object. Applications include imaging and display of three-dimensional (3D) objects, and encryption and pattern recognition of two-dimensional (2D) and 3D objects. Often, these optical systems employ discrete spatial light modulators (SLMs) such as liquid-crystal displays. In the 2D case, SLMs can encode the inputs and keys during encryption and decryption. For 3D processing, the SLM can be used as part of an optical reconstruction technique for 3D objects, and can also represent the key during encryption and decryption. However, discrete SLMs can represent only discrete levels of data necessitating a quantisation of continuous valued analog information. To date, many such optical systems have been proposed in the literature, yet there has been relatively little experimental evaluation of the practical performance of discrete SLMs in these systems. In this paper, we characterise conventional phase-modulating liquid-crystal devices and examine their limitations (in terms of phase quantisation, alignment tolerances, and nonlinear response) for the encryption of 2D and 3D data. Finally, we highlight the practical importance of a highly controlled discretisation (optimal quantisation) for compression of digital holograms.

Keywords: digital holography, optical encryption, quantization, spatial light modulator, image compression, three-dimensional image processing

1. INTRODUCTION

Digital holography[1–8] is an inherently three-dimensional (3D) technique for the capture of real-world objects. Many existing 3D imaging and processing techniques are based on the explicit combination of several two-dimensional (2D) perspectives (or light stripes, etc.) through digital image processing. The advantage of recording a hologram is that multiple 2D perspectives can be optically combined in parallel, and in a constant number of steps independent of the hologram size. Although holography and its capabilities have been known for many decades, digital holography has seen renewed interest due to the recent development of megapixel digital sensors with sufficient spatial resolution and dynamic range. The applications of digital holography could include 3D television, virtual reality, and medical imaging.

One such application of digital holography is optical encryption[9–20] which often produces a complex-valued encrypted image resulting from a random phase mask positioned in the input, Fresnel, or Fraunhofer domain, or combination of domains. Digital holography has been applied to the encryption of 2D conventional (real-valued) images.[15–17] Of these, the techniques based on phase-shift interferometry[3, 5, 8] (PSI) make good use of detector resources in that they capture on-axis encrypted digital holograms.[16, 17] The PSI technique has also been extended to the encryption of 3D objects.[18] The advantage of digital techniques over holographic encryption methods that use more traditional photorefractive media[12, 13] is that the resulting encrypted hologram can be easily stored, processed, and analysed electronically, and transmitted over conventional communication channels.

Corresponding author: tom.naughton@nuim.ie

Often, spatial light modulators (SLMs) such as a liquid-crystal display (LCD) panels are used to encode the inputs and keys in the encryption and decryption stages. There have been three main approaches to represent complex-valued data on a SLM. The first is to map the values to be represented on to the values that a SLM can represent using a minimum Euclidean distance method.[21] The second approach referred to as pseudorandom encoding,[22] statistically approximates the desired complex values with those values that are achievable with a given SLM. Originally developed for phase-only modulators, pseudorandom encoding has been extended to modulators for which amplitude is a function of phase by transforming the phase statistics to compensate for the amplitude coupling. The third approach is to encode the complex valued data as a computer generated hologram[23] (CGH) by using a group of pixels to represent a complex datum. Compared to the CGH approach, the pseudorandom encoding method is a point oriented encoding method and uses the full available space-bandwidth product of the SLM.

To date, many optical systems of this type have been proposed in the literature, yet there has been relatively little experimental evaluation of the practical performance of SLMs in encryption systems. Complex-valued data, when represented on a SLM with a discrete number of levels, leads to quantisation errors. For a double random phase encoding system,[10] Javidi et al.[24] and Goudail et al.[25] have studied how encrypted image perturbations affect the decrypted image. Treatments of quantisation in holograms can be found in the literature,[26, 27] and quantisation of real-valued[28] and complex-valued[29–32] digital holograms, including encrypted digital holograms, has been studied in the context of data compression. A desirable feature when using a SLM for encryption and pattern recognition applications is a large space-bandwidth product (number of pixels in the SLM). This often means a reduction in pixel size, making the optical system less tolerant to misalignment errors of the SLM. Recently, Unnikrishnan et al.[12] have studied the effects of SLM misalignment in a double random phase encoding system.

In this paper, we consider optical systems that encrypt 2D and 3D objects. Our 3D objects are captured using in-line phase-shift digital interferometry.[8, 33, 34] In addition to amplitude, optical systems offer many degrees of freedom to encode data such as phase,[10, 12, 19, 32, 35, 36] polarization,[37] and wavelength.[13] In our system, the encryption is performed using a random phase mask in a Fresnel plane. The random phase mask, acting as the encryption/decryption key, is displayed on a SLM. The large space bandwidth product of the SLM means that key sizes in the order of hundreds of thousands or even millions of digits are feasible. The encrypted data captured by the CCD camera is a complex-valued white-noise-like signal. When decrypting, the complex-valued data (or some real function of it) is displayed on the first SLM and the decoding mask is displayed on the second SLM. We use a virtual optics method to simulate the encryption and decryption process. The efficient linear canonical transform (LCT) algorithm proposed by Hennelly and Sheridan[38] could simulate any such optical system. The display of the encrypted image and decoding mask on SLMs results in quantisation depending on the number of discrete amplitude or phase levels offered by each SLM.

We characterise conventional phase-modulating liquid-crystal devices and examine their limitations (in terms of phase quantisation, alignment tolerances, and nonlinear response) in the context of 2D and 3D optical encryption and decryption. At the decryption side, it is usual for the complex-valued encrypted image to be displayed on one or more SLMs and propagated through a decryption system. A similar phase-only optical system has been proposed and demonstrated for the optical reconstruction of 3D objects encoded in digital holograms.[30] In this paper, we consider the effects of phase quantisation and nonlinear SLM response in such an optical reconstruction system. Also, we highlight the practical importance of highly controlled discretisation for compression of digital holograms. This will in general be a nonuniform quantisation and it assumes an ideal SLM. We present the results of one such popular technique (k-means clustering) and compare it to a more computationally efficient technique that we have implemented: what in communication theory is known as optimal signal quantisation.[39]

This paper is organised as follows. In Sect. 2 we explain our encryption and decryption mechanism, and in Sect. 3 explain our method for measuring quantisation and misalignment tolerances. The results of our investigations into SLM quantisation and SLM misalignment are presented in Sects. 4 and 5, respectively. In this latter section, too, we characterise the nonlinear response of our phase-modulating SLM and investigate the optical encryption system's tolerance to the unwanted amplitude modulation that is coupled with each phase level. We illustrate the use of nonuniform quantisation for digital hologram compression in Sect. 6, and conclude in Sect. 7.
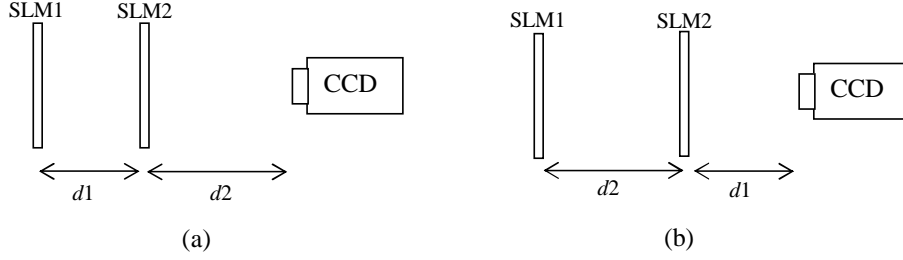
Figure 1. Schematic of the optical system for encryption and decryption.

2. ENCRYPTION AND DECRYPTION

In this section, we describe the process of encryption and decryption of the data. The following analysis is carried out in one dimension with extension to two dimensions straightforward. Let $f(x)$ represent the input data to be encrypted. Let $L_{\alpha1,\beta1,\gamma1}$ and $L_{\alpha2,\beta2,\gamma2}$ represent LCTs corresponding to two combinations of lenses and free space propagation distances. The input signal $f(\cdot)$ is transformed using $L_{\alpha1,\beta1,\gamma1}$, multiplied by a random phase mask R and transformed again using $L_{\alpha2,\beta2,\gamma2}$.

The LCT $L_{\alpha,\beta,\gamma}$ of $f(\cdot)$ is a three parameter transform described as

$$L_{\alpha,\beta,\gamma}[f](x') = K \iint f(x) \exp\left[j\pi(\alpha x^2 - 2\beta x x' + \gamma x'^2)\right] \mathrm{d}x. \tag{1}$$

The encrypted signal $\Psi(\cdot)$ can be written as

$$\Psi(\cdot) = L_{\alpha2,\beta2,\gamma2}[L_{\alpha1,\beta1,\gamma1}(f)R], \tag{2}$$

and could be decrypted with

$$f(\cdot) = L_{-\alpha1,-\beta1,-\gamma1}\{R^* L_{-\alpha2,-\beta2,-\gamma2}[\Psi(\cdot)]\}, \tag{3}$$

where $L_{-\alpha,-\beta,-\gamma}$ is the inverse transform of $L_{\alpha,\beta,\gamma}$ and $*$ indicates complex conjugate. There is a second method of decryption, suitable for optical implementation, using the following property of LCT

$$L_{-\alpha,-\beta,-\gamma}(f) = [L_{\alpha,\beta,\gamma}(f^*)]^*. \tag{4}$$

Using this property, we can write Eq. 3 as

$$f^*(\cdot) = L_{\alpha1,\beta1,\gamma1}\{R L_{\alpha2,\beta2,\gamma2}[\Psi^*(\cdot)]\}. \tag{5}$$

If $f(\cdot)$ is real, $f^*(\cdot) = f(\cdot)$. If one takes the conjugate of the encrypted signal and does the LCT operations used for encryption in reverse order, one gets the conjugate of the input signal. In the present work, $L_{\alpha1,\beta1,\gamma1}$ and $L_{\alpha2,\beta2,\gamma2}$ corresponds to free space distances d_1 and d_2 in which case

$$\alpha1 = \beta1 = \gamma1 = \frac{\pi}{\lambda d_1}, \alpha2 = \beta2 = \gamma2 = \frac{\pi}{\lambda d_2}, \tag{6}$$

where λ is the wavelength of light used.

In our experiments, we used digitised photographs as our 2D objects. The phase mask consisted of values chosen with uniform probability from the range $[0, 2\pi)$ using a pseudo-random number generator. Digital holograms of 3D objects were captured using an in-line PSI set-up[33, 34] based on a Mach-Zehnder interferometer. Encrypted versions of these holograms can be obtained by positioning the phase mask between the object and the digital camera. For our experiments, this encryption step was simulated[32] after optical capture of the real-world 3D objects.

3. QUANTISATION AND MISALIGNMENT ERRORS DUE TO SLM

Figure 1 shows the optical system used for encryption and decryption. In Fig. 1(a), SLM1 and SLM2 are used to display the input image and encryption key, respectively. In Fig. 1(b), SLM1 and SLM2 are used to display the encrypted image and the decryption key, respectively. We perform the encryption and decryption process by a virtual optics method using the discrete Fresnel transform, which is a special case of the discrete LCT and for which efficient $n \log(n)$ time algorithms exist.[38] The wavelength of the coherent source was $532 \, \text{nm}$, the distances d_1 and d_2 were $80 \, \text{mm}$, the CCD pixel size was $9 \, \mu\text{m}$ and the SLM pixel size was $36 \, \mu\text{m}$. We assumed a 100% fill factor for both the SLM and CCD.

The error in the decoded image when the SLM is used to represent the encrypted image is studied by modifying the encrypted image according to

$$\Psi_i' = \Psi_i + \Delta\Psi_i \,, \tag{7}$$

where Ψ_i represents the value of the ith pixel in the encrypted image, Ψ_i' represents the corresponding value represented by the SLM, and $\Delta\Psi_i$ is the resulting quantisation error for that pixel. If a_i represents the amplitude and ϕ_i represents the phase of each quantised complex value Ψ_i' then $a_i \in \{a^1 \ldots a^n\}$ for n predefined amplitude levels and $\phi_i \in \{\phi^1 \ldots \phi^n\}$ for n predefined phase levels. The error r in the decoded image is calculated using a normalised rms (NRMS) error metric defined as

$$r = \left(\sum_{i=1}^{N} \sum_{j=1}^{N} |I_\text{d}(i,j) - I(i,j)|^2 \right)^{\frac{1}{2}} \left(\sum_{i=1}^{N} \sum_{j=1}^{N} |I(i,j)|^2 \right)^{-\frac{1}{2}} , \tag{8}$$

where $I_\text{d}(\cdot)$ and $I(\cdot)$ are the intensities of the decrypted and original images, respectively.

To study the error in the decoded image when a SLM is used to represent the decryption mask the decryption mask R' is modified to conform to

$$R_i' = \exp(\text{i}\theta_i) \tag{9}$$

for each pixel i, where $\theta_i \in \{\theta^1 \ldots \theta^n\}$ for n discrete phase levels. The sensitivity of the position of the mask in the decryption process is studied by misaligning the decryption mask by a fraction of a pixel in transverse x, y and longitudinal z directions, according to

$$R'(x', y', z') = R(x + \Delta x, y + \Delta y, z + \Delta z) \,, \tag{10}$$

where Δx, Δy, and Δz are the misalignments (in units of pixels) in the transverse x, y and longitudinal z directions, respectively.

4. PHASE QUANTISATION

In this section we present some results from our simulation study. Figure 2(a) shows the 512×512 pixel greyscale 2D image used in our study. We corrupted the 2D image with random phase to make it correspond to the full Fresnel field immediately in front of a reflective real-world object. The image was encrypted as described in Sect. 2. The encryption phase mask had 256 discrete levels. First we studied the quantisation effect of the phase-only SLM displaying the decoding phase mask. The phase of the decrypting phase mask is quantised to different numbers of discrete levels. Figures 2(b) through (d) show the decrypted image when the phase mask is quantised to various numbers of levels.

Next we studied the effects due to the finite number of discrete levels of the SLM displaying the encrypted image. We do not consider the amplitude of the encrypted image and consider only the phase; we assume that we have access only to a phase-only SLM. (This amplitude removal or amplitude equalisation concept has been shown to be a useful low-cost technique for the reconstruction of digital holograms using phase-only SLMs.[30]) The phase of the encrypted image was quantised to different numbers of levels ranging from 2 to 256. Several of these decrypted images are shown in Fig. 3. Plots of NRMS error as a function of phase levels for each of these two simulation studies are shown in Fig. 4. It was found that the error increases dramatically when the number of phase levels falls below 10 in each case. In Fig. 4(b) the error never falls below approximately 0.4 even when no phase quantisation is applied. This has been noticed before in relation to digital holograms[30] and corresponds to the fundamental losses introduced by amplitude equalisation.

Figure 2. The decrypted 2D image with (a) no quantisation, and decrypted with (b) 64, (c) 8, and (d) 2 quantisation levels in the phase mask.

Figure 3. The decrypted 2D image after the phase-only encrypted image is quantised to (a) 128, (b) 8, (c) 4, and (d) 2 phase levels.
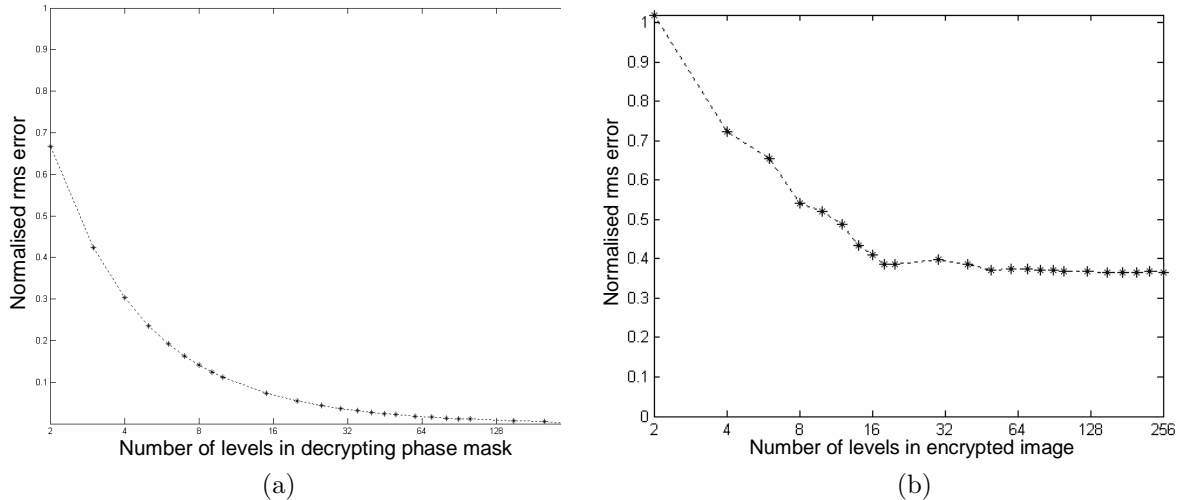
Figure 4. Plots showing (a) NRMS error as a function of number of quantisation levels in the decrypting phase mask, and (b) NRMS error as a function of number of quantisation levels in the SLM displaying the phase-only information of the encrypted image. Each plot has a logarithmic scale in its horizontal axis.

5. MISALIGNMENT AND NONLINEAR RESPONSE

Our third study concerns errors introduced due to in-plane misalignment of the decoding phase mask and misalignment along the optical axis. Figure 5(a) and (b) show the results of horizontal misalignment, (c) and (d) show the results of vertical misalignment, and (e) and (f) show the results of longitudinal misalignment. The error introduced by misalignment of the decrypting phase mask in each of these three directions is plotted in Fig. 6 for different values ranging from $-1\,\text{mm}$ to $1\,\text{mm}$. It can be noted from the plot that the decryption system is more sensitive to misalignment in the transverse (in-plane) direction than in the longitudinal direction (along the optical axis).

Our fourth study concerned the non-ideal response of our SLM. A Mach-Zehnder interferometer was used to characterise our LCD SLM. When in phase-modulating mode, the SLM was found to give a phase modulation in the interval $[0, 2\pi]$. However, the amplitude varied over this range. As the polar plot shows in Fig. 7 the SLM was found to work in a coupled mode; an undesirable amplitude modulation was coupled with the phase modulation. The actual response differs to the ideal response in two respects. Firstly, the SLM has a nonlinear phase response to grey level input. This is evident from the nonuniform spacing between points on the curve. Secondly, there is the undesirable coupled amplitude modulation which results in errors in the decryption and reduces the overall light efficiency of the system. When employing this SLM response data for later experiments we let our 26 sample measurements correspond to 26 discrete levels of phase quantisation.

We evaluated the effect on a 3D optical encryption system of such a non-ideal SLM. Several 3D objects were captured with phase-shift digital holography based on a Mach-Zehnder interferometer architecture.[33, 34] The 1024×1024 pixel complex-valued digital holograms were retrospectively encrypted in software using a phase mask in the Fresnel domain[32] as illustrated in Fig. 1. We encrypted the objects using an idealised phase-only SLM without quantisation for the encryption phase mask. Decryption experiments with three different phase mask SLMs were performed for each object. First, we decrypted the objects using an idealised SLM without quantisation to determine the highest quality decrypted reconstructions possible. Next, we decrypted the objects using an idealised phase-only SLM with the 26 discrete phase levels shown in Fig. 7. Finally, we decrypted the objects using the actual coupled-mode response shown in Fig. 7. These three reconstructions for two of our 3D objects are shown in Figs. 8 and 9. Each reconstruction was mean filtered with a 5×5 pixel neighbourhood prior to NRMS error calculation to reduce the disparity between the unique speckle patterns generated in each reconstruction.
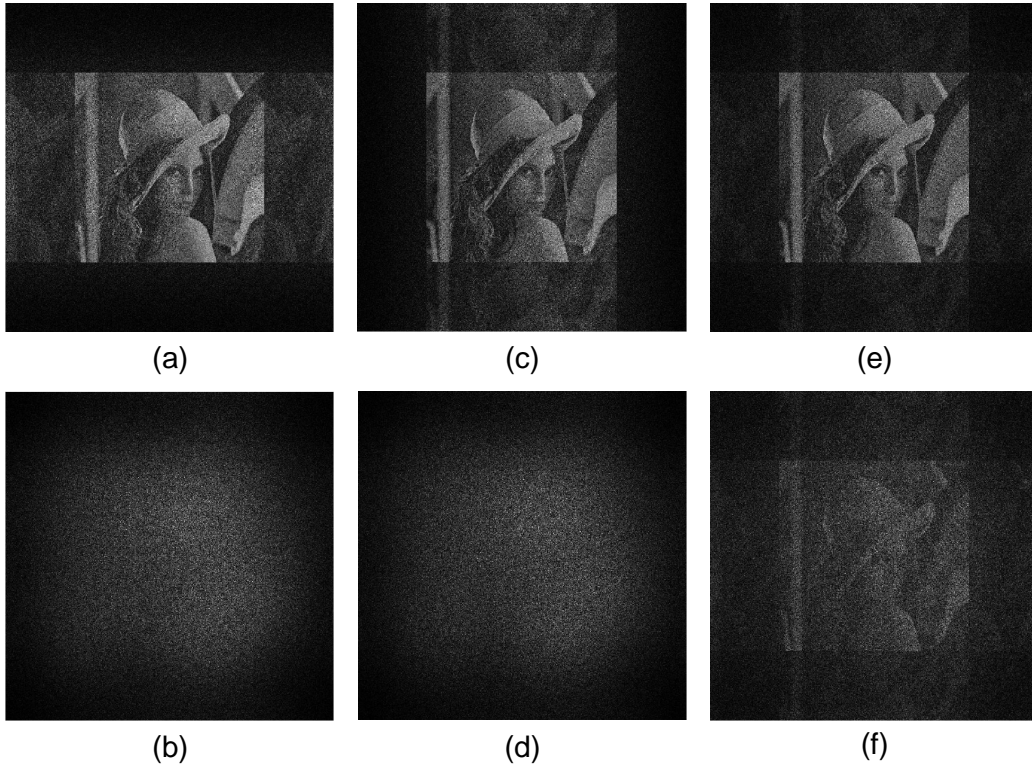
Figure 5. Decrypted image when the decrypting phase mask is out of alignment by (a) 0.009 mm and (b) 0.036 mm in the horizontal transverse direction, (c) 0.009 mm and (d) 0.036 mm in the vertical transverse direction, and (e) 0.5 mm and (f) 1.0 mm in the longitudinal (along the optical axis) direction.
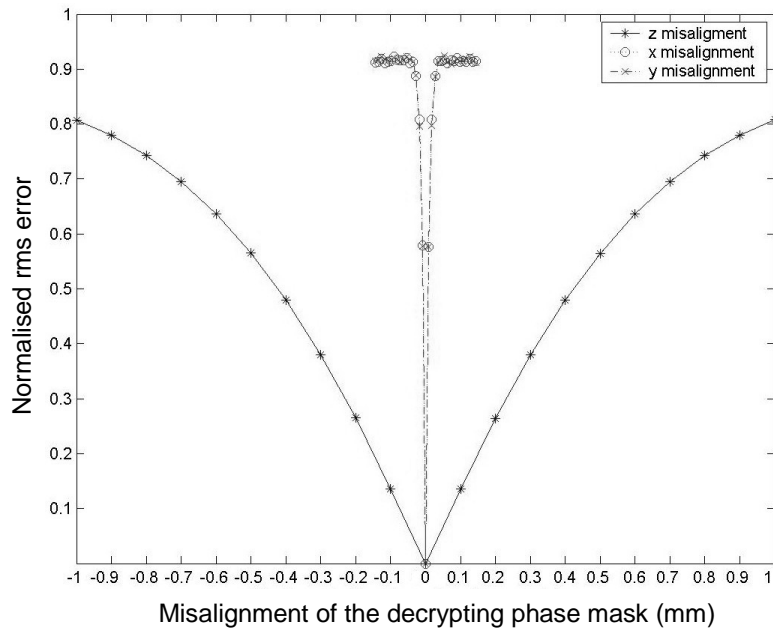

Figure 6. NRMS error as a function of the misalignment of the decrypting phase mask in both transverse (x and y in the plot) directions and along the optical axis (y).
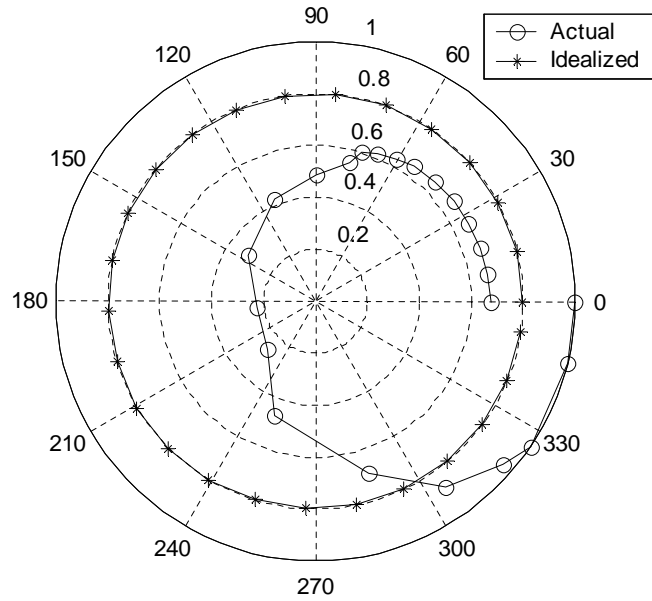
Figure 7. Polar plot of normalised amplitude against phase angle. Plot shows the actual response of the SLM for input grey levels varying from 0 to 255 in quantisation steps of 10 levels (some points are coincident), and an idealised response with constant amplitude of 0.8.
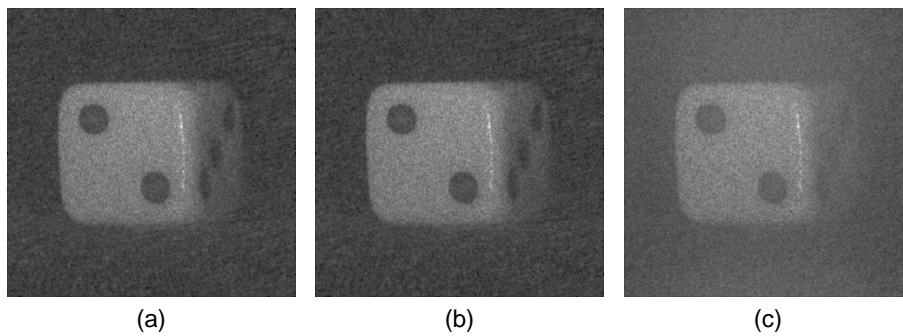

Figure 8. Decryption and reconstruction of a 3D object using a phase mask displayed on (a) an idealised phase-only SLM without quantisation (NRMS error 0.0), (b) an idealised phase-only SLM with quantisation as shown in Fig. 7 (NRMS error 0.017), and (c) a SLM with the quantised coupled-mode response shown in Fig. 7 (NRMS error 0.65).
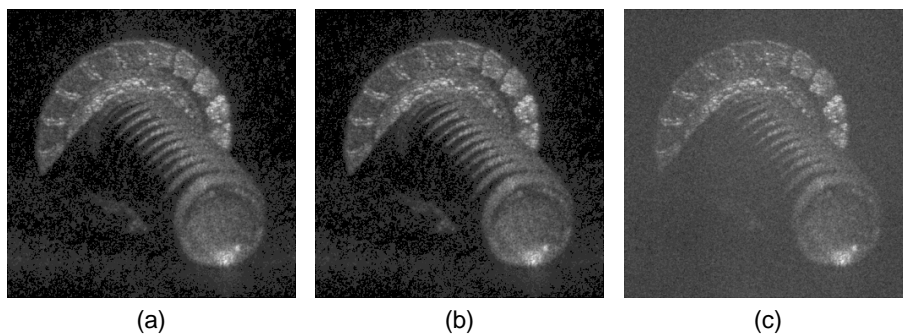

Figure 9. Decryption and reconstruction of a 3D object using a phase mask displayed on (a) an idealised phase-only SLM without quantisation (NRMS error 0.0), (b) an idealised phase-only SLM with quantisation as shown in Fig. 7 (NRMS error 0.01), and (c) a SLM with the quantised coupled-mode response shown in Fig. 7 (NRMS error 0.70).
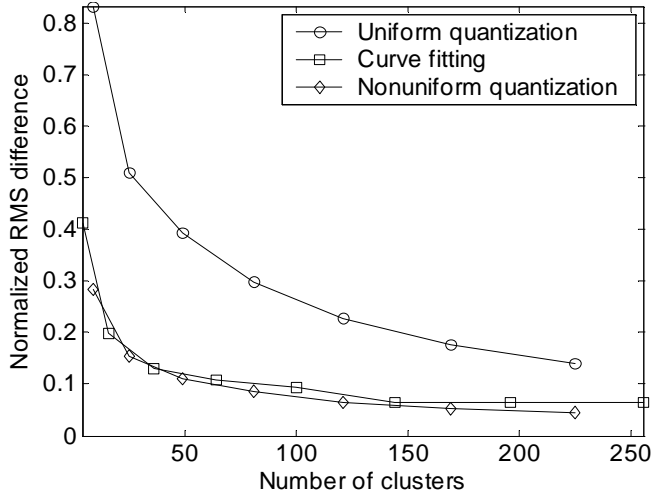
Figure 10. NRMS difference in the reconstructed object plotted against number of clusters for uniform quantisation, optimal quantisation applied to the Gaussian approximations of our real and imaginary hologram data and k-means nonuniform quantisation in the 3D object shown in Fig. 9.

6. NONUNIFORM QUANTISATION FOR DATA COMPRESSION

The phase quantisation effect from our actual SLM characterisation outlined in the previous section can be referred to as nonuniform quantisation: the discrete levels were not uniformly distributed in phase space. Nonuniform quantisation is a promising candidate for a digital hologram compression technique. Quantisation and phase quantisation have been applied successfully to Fourier and holographic data in the past.[27–32] Here, we choose optimal nonuniform distributions of quantisation values. The technique we apply was initially developed for optimal quantisation of signals.[39] It was later used for quantisation of Fourier spectra for digital hologram applications[40] and has also been used in the design of an optimally quantised phase-only matched filter for image recognition.[41] Time- and space-efficient digital hologram compression algorithms enable applications that rely on the efficient storage and transmission of 3D objects.[31]

The optimal quantisation technique for 1D signals has a straightforward iterative algorithm.[39] Our digital hologram data is amenable to quantization using this technique because it has to a good approximation a normal distribution of real and imaginary values. We decompose our digital holograms into a histogram of real values and a histogram of imaginary values, and fit gaussians to these 1D signals. We find the optimal quantisation for $\sqrt{N}$ levels in each gaussian curve and pair them to obtain N complex-valued cluster centres. The digital holograms are quantized by setting each of their complex-valued pixels to the closest cluster centre. Employing a higher number of cluster centres will increase the reconstruction quality but lower the compression ratio. The resulting reconstruction NRMS errors for our curve fitting optimal quantisation approach are shown in Fig. 10. We compare our technique to uniform quantisation and the popular k-means nonuniform clustering algorithm. It can be seen that the k-means algorithm and optimal quantization perform equally well. From this plot, one can see that the reconstruction errors remain manageable for as few as 25 clusters. This corresponds to 5 quantisation levels in each of the real and imaginary parts of each holographic pixel. If the original data has 8 bits of information in each real and imaginary stream, this corresponds to a compression ratio of 50. Lossless compression techniques could subsequently be employed to reduce this compression ratio even further.

7. CONCLUSION

In this paper, we simulate the encryption and decryption of 2D and 3D objects. Our 3D objects are real-world objects captured using phase-shift digital holography. Encryption is performed with a phase mask in the Fresnel domain. The specific case of a phase-only SLM is studied. We study the sensitivity of the decoding system to the finite phase quantisation of the SLM used to represent the encrypted image and the decoding mask. The tolerances of the system to 3D misalignment errors of the SLM used to represent the decoding mask are also

studied. We used only the phase information of the encrypted image for decryption, and noted the importance of this phase information and that some information is fundamentally lost when the amplitude is equalised. Phase-only SLMs are useful for real-time reconstruction of 3D digital holograms, and these issues have also been discussed by Matoba et al.[30] in this context. We demonstrate that a SLM which can produce at least 10 discrete phase levels in the $[0, 2\pi]$ interval can be productively employed in optical systems to encrypt/decrypt images. The higher the space-bandwidth product of the SLM, the more sensitive is the optical system to misalignment errors of the SLM particularly in the transverse direction to the optical axis of the system.

As well as being an undesirable property of SLMs for encryption, decryption, and display, quantisation is an important consideration for real-time 3D applications. Combined with quantisation compression, the optical encryption technique based on phase-shift digital holography is suitable for a range of secure and efficient 3D object storage and transmission applications. It can be seen that the k-means algorithm and optimal quantization perform equally well on our encrypted 3D digital holograms. If one has a priori knowledge of the distribution of one's data, as we have to a large extent with our digital hologram data, then the optimal technique would be preferable due to its lower computational complexity.

ACKNOWLEDGEMENTS

REFERENCES

1. J. W. Goodman and R. W. Lawrence, "Digital image formation from electronically detected holograms," *Applied Physics Letters* **11**(2), pp. 77–79, 1967.
2. L. P. Yaroslavskii and N. S. Merzlyakov, *Methods of Digital Holography*, Consultants Bureau, Plenum, New York, 1980. Translated from Russian by Dave Parsons.
3. J. H. Bruning, D. R. Herriott, J. E. Gallagher, D. P. Rosenfeld, A. D. White, and D. J. Brangaccio, "Digital wavefront measuring interferometer for testing optical surfaces and lenses," *Applied Optics* **13**, pp. 2693–2703, Nov. 1974.
4. T.-C. Poon and A. Korpel, "Optical transfer function of an acousto-optic heterodyning image processor," *Optics Letters* **4**, pp. 317–319, 1979.
5. J. Schwider, B. Burow, K. E. Elsner, J. Grzanna, and R. Spolaczyk, "Digital wavefront measuring interferometry: some systematic error sources," *Applied Optics* **22**, pp. 3421–3432, 1983.
6. L. Onural and P. D. Scott, "Digital decoding of in-line holograms," *Opt. Eng.* **26**, pp. 1124–1132, 1987.
7. U. Schnars and W. P. O. Jüptner, "Direct recording of holograms by a CCD target and numerical reconstruction," *Applied Optics* **33**, pp. 179–181, Jan. 1994.
8. I. Yamaguchi and T. Zhang, "Phase-shifting digital holography," *Optics Letters* **22**, pp. 1268–1270, 1997.
9. B. Javidi and J. L. Horner, "Optical pattern recognition for validation and security verification," *Optical Engineering* **33**, pp. 1752–1756, June 1994.
10. P. Réfrégier and B. Javidi, "Optical image encryption based on input plane and Fourier plane random encoding," *Optics Letters* **20**, pp. 767–769, Apr. 1995.
11. L. G. Neto and Y. Sheng, "Optical implementation of image encryption using random phase encoding," *Optical Engineering* **35**(9), pp. 2459–2463, 1996.
12. G. Unnikrishnan, J. Joseph, and K. Singh, "Optical encryption system that uses phase conjugation in a photorefractive crystal," *Applied Optics* **37**, pp. 8181–8186, Dec. 1998.
13. O. Matoba and B. Javidi, "Encrypted optical memory system using three-dimensional keys in the Fresnel domain," *Optics Letters* **24**, pp. 762–764, June 1999.
14. P. C. Mogensen and J. Glückstad, "Phase-only optical encryption," *Optics Letters* **25**, pp. 566–568, Apr. 2000.
15. B. Javidi and T. Nomura, "Securing information by use of digital holography," *Optics Letters* **25**, pp. 28–30, Jan. 2000.

16. S. Lai and M. A. Neifeld, "Digital wavefront reconstruction and its application to image encryption," *Optics Communications* **178**, pp. 283–289, May 2000.
17. E. Tajahuerce, O. Matoba, S. C. Verrall, and B. Javidi, "Optoelectronic information encryption with phase-shifting interferometry," *Applied Optics* **39**, pp. 2313–2320, May 2000.
18. E. Tajahuerce and B. Javidi, "Encrypting three-dimensional information with digital holography," *Applied Optics* **39**, pp. 6595–6601, Dec. 2000.
19. B. M. Hennelly and J. T. Sheridan, "Optical image encryption by random shifting in fractional Fourier domains," *Optics Letters* **28**, pp. 269–271, Feb. 2003.
20. N. K. Nishchal, J. Joseph, and K. Singh, "Fully phase encryption using fractional Fourier transform," *Optical Engineering* **42**, pp. 1583–1588, June 2003.
21. R. D. Juday, "Optimal realizable filters and the minimum Euclidean distance principle," *Applied Optics* **32**, pp. 5100–5111, 1993.
22. R. W. Cohn, "Pseudorandom encoding of complex-valued functions onto amplitude-coupled phase modulators," *Journal of the Optical Society of America A* **15**, pp. 868–883, 1998.
23. P. M. Birch, R. Young, D. Budgett, and C. Chatwin, "Two-pixel computer-generated hologram with a zero-twist nematic liquid-crystal spatial light modulator," *Optics Letters* **25**, pp. 1013–1015, 2000.
24. B. Javidi, A. Sergent, G. Zhang, and L. Guibert, "Fault tolerance properties of a double phase encoding encryption technique," *Optical Engineering* **36**, pp. 992–998, 1997.
25. F. Goudail, F. Bollaro, B. Javidi, and P. Réfrégier, "Influence of a perturbation in a double phase-encoding system," *Journal of the Optical Society of America A* **15**, pp. 2629–2638, 1988.
26. J. W. Goodman and A. M. Silvestri, "Some effects of Fourier domain phase quantization," *IBM J. Res. Develop.* **14**, pp. 478–484, Sept. 1970.
27. W. J. Dallas and A. W. Lohmann, "Phase quantization in holograms – depth effects," *Applied Optics* **11**, pp. 192–194, Jan. 1972.
28. T. Nomura, A. Okazaki, M. Kameda, Y. Morimoto, and B. Javidi, "Digital holographic data reconstruction with data compression," in *Algorithms and Systems for Optical Information Processing V*, B. Javidi and D. Psaltis, eds., *Proceedings of SPIE vol. 4471*, pp. 235–242, (San Diego, California), July 2001.
29. T. J. Naughton, Y. Frauel, B. Javidi, and E. Tajahuerce, "Compression of digital holograms for three-dimensional object reconstruction and recognition," *Applied Optics* **41**, pp. 4124–4132, July 2002.
30. O. Matoba, T. J. Naughton, Y. Frauel, N. Bertaux, and B. Javidi, "Real-time three-dimensional object reconstruction by use of a phase-encoded digital hologram," *Applied Optics* **41**, pp. 6187–6192, Oct. 2002.
31. T. J. Naughton, J. B. McDonald, and B. Javidi, "Efficient compression of Fresnel fields for Internet transmission of three-dimensional images," *Applied Optics* **42**, pp. 4758–4764, Aug. 2003.
32. T. J. Naughton and B. Javidi, "Compression of encrypted three-dimensional objects using digital holography," *Optical Engineering* **43**, pp. 2233–2238, Oct. 2004.
33. B. Javidi and E. Tajahuerce, "Three-dimensional object recognition by use of digital holography," *Optics Letters* **25**, pp. 610–612, May 2000.
34. Y. Frauel, E. Tajahuerce, M.-A. Castro, and B. Javidi, "Distortion-tolerant three-dimensional object recognition with digital holography," *Applied Optics* **40**, pp. 3887–3893, Aug. 2001.
35. G. Unnikrishnan, J. Joseph, and K. Singh, "Optical encryption by double-random phase encoding in the fractional Fourier domain," *Optics Letters* **25**, pp. 887–889, June 2000.
36. B. M. Hennelly and J. T. Sheridan, "Random phase and jigsaw encryption in the Fresnel domain," *Optical Engineering* **28**, Oct. 2004.
37. G. Unnikrishnan, M. Pohit, and K. Singh, "A polarization encoded optical encryption system using ferroelectric spatial light modulator," *Optics Communications* **185**, pp. 25–31, 2000.
38. B. M. Hennelly and J. T. Sheridan, "Fast numerical algorithm for the linear canonical transform," *Journal of the Optical Society of America A* **22**, May 2005.
39. J. Max, "Quantizing for minimum distortion," *IRE Trans. Information Theory* **IT-6**, pp. 7–12, 1960.
40. N. C. Gallagher, "Optimum quantization in digital holography," *Applied Optics* **17**(1), pp. 109–115, 1978.
41. V. Kober, L. P. Yaroslavsky, J. Campos, and M. J. Yzuel, "Optimal filter approximation by means of a phase-only filter with quantization," *Optics Letters* **19**, pp. 978–980, July 1994.